PHYSICAL REVIEW C, VOLUME 65, 021601(R)

^{239}Pu$(n,2n)^{238}$Pu cross section deduced using a combination of experiment and theory

L. A. Bernstein, J. A. Becker, P. E. Garrett, W. Younes, D. P. McNabb, D. E. Archer, C. A. McGrath,* H. Chen, W. E. Ormand, and M. A. Stoyer
Lawrence Livermore National Laboratory, Livermore, California 94551

R. O. Nelson, M. B. Chadwick, G. D. Johns, W. S. Wilburn, M. Devlin, D. M. Drake, and P. G. Young
Los Alamos National Laboratory, Los Alamos, New Mexico 87545

(Received 23 July 2001; published 9 January 2002)

The ^{239}Pu$(n,2n)^{238}$Pu cross section has been deduced using a combination of measured partial γ-ray cross sections and enhanced Hauser-Feshbach reaction modeling from threshold to $E_n \leqslant 20$ MeV. Eight ^{239}Pu$(n,2n\gamma)^{238}$Pu partial γ-ray cross sections were measured using the GEANIE spectrometer, the time-of-flight technique, and energetic neutrons produced at the LANSCE/WNR facility. The $(n,2n)$ cross section was obtained by multiplying the sum of observed noncoincident partial γ-ray cross sections by the calculated ratio of the $(n,2n)$ cross section divided by the sum of the same partial γ-ray cross sections. A comparison between the data and model calculations indicates potential deficiencies in the modeling of the γ-ray cascade.

DOI: 10.1103/PhysRevC.65.021601 PACS number(s): 25.40.−h, 28.20.−v, 21.10.−k, 25.40.Fq

Efforts to measure the ^{239}Pu$(n,2n)$ cross section over the past three decades have faced formidable challenges, most notably the competition with fission. Prompt neutron measurements [1,2] as a function of incident neutron energy are complicated by the presence of a large (2+ barns) fission channel which produces on average 3–4 neutrons. The most accurate measurement performed to date of the cross section involved α-decay counting of a ^{239}Pu sample that initially contained less than one part in 10^9 of ^{238}Pu following irradiation using an intense 14 MeV D-T neutron source [3].

This Rapid Communication reports the measurement of prompt γ-ray cross sections in ^{238}Pu over a wide range of incident neutron energies using a high-resolution $(\Delta E_\gamma/E_\gamma)$ γ-ray spectrometer coupled to a pulsed ''white'' neutron source. The $(n,2n)$ cross section is obtained by multiplying measured γ-ray partial cross sections by the calculated ratio of the $(n,2n)$ cross section to the partial γ-ray cross sections obtained from a Hauser-Feshbach based reaction model [4]. The model provides the ''missing'' γ-ray intensity that does not produce observed γ rays while the measurement removes the uncertainty in the model calculation arising from the uncertainties in the total reaction cross section.

Several examples exist in the literature where partial γ-ray cross sections were used to estimate channel cross sections where the majority of the γ-ray intensity was observed or there was no competition from other channels [5]. In 1994 Vonach *et al.* [6] suggested that partial γ-ray cross sections could be converted into a channel cross section through the use of reaction modeling. The work presented here is the first attempt at performing this transformation where there are strong competing channels and numerous γ-ray decay paths at low excitation energies in the residual nucleus. This technique provides a new means to determine reaction cross sections where conventional measurements are intractable.

Neutrons were produced from the Weapons Neutron Research (WNR) facility at the Los Alamos Neutron Science Center (LANSCE) [7] spallation source. The time structure of the proton beam ($I_{average} = 2-6\ \mu A$) consisted of 100–119 ''macropulses'' per second, each 625–750 μs in length, providing an overall duty cycle of $\approx 6-7$ %. These macropulses were composed of ''micropulses,'' spaced every 1.8 μs, thereby allowing for determination of E_n from the time of flight. In-beam and beam-off γ rays were detected using the GEANIE spectrometer. GEANIE is composed of 15 coaxial Ge detectors (nine suppressed) and 11 planar Compton suppressed Ge detectors. The spectrometer and the experimental setup are described in greater detail in the references [8]. A target of 98.014% enriched ^{239}Pu [9] with thickness of 0.0277(8) cm (thin) or alternatively 0.0500(3) cm (thick) was placed in the array center of a distance of 20.34 m from the spallation target. Neutron fluences were measured with ^{235}U and ^{238}U fission chambers located 18.48 m from the spallation target.

In-beam recorded data consisted of γ-ray pulse heights with 20 keV$\leqslant E_\gamma \leqslant$1 MeV for the planar and 50 keV$\leqslant E_\gamma \leqslant$4 MeV for the coaxial detectors, together with correlated event time relative to the beam micropulse time. Scalar data were recorded to allow determination of the system deadtime. The array efficiency was measured using a set of calibration sources. MCNP calculations [10] that reproduced the source data were used to interpolate between discrete γ-ray energies and to correct for beam profile and target geometry effects [11]. Data representing a total of 24 and 12 d of beam-time were collected on the thin and thick targets, respectively. An overall check at $E_\gamma = 846.8$ keV was obtained by placing a pair of 8×10^6 $^{\text{nat}}$Fe foils on either side of the ^{239}Pu target during one of the irradiations. The measured partial γ-ray cross section for the ^{56}Fe $2_1^+ \rightarrow 0_1^+$ transition was extracted from the data to be 862.6(10.0) mb at $E_n = 13.9(0.6)$ MeV, in excellent agreement with the tabulated value of 855(51) mb at 14.5 MeV [12].

A brief overview of the data analysis procedure is presented here (more details can be found in Ref. [13]). The LEPS data were the primary focus of the analysis for $E_n \leqslant 1$ MeV due to their superior energy resolution and peak-

*Present address: Idaho National Engineering and Environmental Laboratory, P.O. Box 1625, Idaho Falls, ID 83415.

to-background ratios compared to the coaxial detectors. 13 candidate $(n,2n\gamma)$ transitions were identified by their γ-ray energy in a spectrum corresponding to an incident neutron energy between 1 and 25 MeV. A parametrized fit of this γ-ray spectrum was obtained for energies near each candidate γ ray using the GF2 code [14]. γ-ray spectra corresponding to adjacent 20 ns wide time-of-flight bins were formed and the parameters obtained from the $E_n=1-25$ MeV integrated spectrum were used to produce γ-ray yields as a function of E_n. All parameters in the fit were fixed except for the peak heights and the quadratic γ-ray energy background. γ-ray yields (Γ_{yield}) were obtained by dividing the peak areas by the total neutron fluence extracted from an equivalent 20 ns time-of-flight bin from the fission chamber data using (n,f) cross sections from Ref. [15]. The average neutron energy and the uncertainty for each of these bins was calculated taking into account the detector timing response as 10–20 ns. Only eight of the 13 candidate transitions exhibited the correct threshold energy with respect to $E_{th}(n,2n)=5.6$ MeV for assignment to the $(n,2n)$ channel.

The γ-ray yield curves for these eight transitions were converted into partial transition cross sections using the following formula:

$$\sigma_{partial\ \gamma\text{-}ray}=\frac{\Gamma_{yield}}{N_{239\mathrm{Pu}}\times\Phi_{FC}}\times W(\theta)(1+\alpha_{tot})\frac{LT_{\mathrm{Ge}}}{LT_{FC}}\times\frac{1}{\epsilon}, \tag{1}$$

where $N_{239\mathrm{Pu}}$ is the number of ^{239}Pu atoms in the target, Φ_{FC} is the neutron flux as deduced from the fission chamber data, $W(\theta)$ is an angular distribution correction factor, α_{tot} is the electron conversion coefficient, LT_{Ge} and LT_{FC} are the Ge detectors and fission chamber live-times, and ϵ is the efficiency for detecting the γ ray. Conversion coefficients and multipolarity assignments (as well as mixing ratios, when appropriate) used to calculate the cross sections were taken from the National Nuclear Data Center [16].

Cross sections were in good agreement among all of the data sets. The data sets were gain-matched and summed to form one spectrum for each neutron energy cut to minimize statistical uncertainties. Figure 1 shows a region of the summed γ-ray spectrum near the $E_\gamma=157.4$ keV $6^+(E_x=303.4$ keV$)\rightarrow 4^+$ (top) and the $E_\gamma=936.6$ keV $4^-(E_x=1083.0$ keV$)\rightarrow 4^+$ (bottom) γ rays from ^{238}Pu corresponding to a neutron energy of 11.37(45) MeV. The analysis procedure described above was repeated for these summed spectra to produce partial transition cross sections. Figure 2 shows the four strongest transitions in ^{238}Pu observed in the data; the yrast $E_\gamma=157.4$ keV $6^+(E_x=303.4$ keV$)\rightarrow 4^+$, the $E_\gamma=210.0$ keV $8^+(E_x=513.4$ keV$)\rightarrow 6^+$, the $E_\gamma=936.6$ keV $4^-(E_x=1083.0$ keV$)\rightarrow 4^+$, and the $E_\gamma=924.0$ keV $2^-(E_x=968.1$ keV$)\rightarrow 2^+$ transitions. Observation of the two lowest yrast transitions, the $2_1^+\rightarrow 0_1^+$ and $4_1^+\rightarrow 2_1^+$ transitions, was hindered due to internal conversion, attenuation of the γ rays in the target, and contamination from a fission fragment γ ray with the same energy. Several higher energy off-yrast transitions were readily identified in the data in part because they were less susceptible to target attenuation, internal conversion, and background from Compton scattering of ^{239}Pu decay γ rays.

A description of the Hauser-Feshbach reaction models used to extract the channel cross section is given next. The GNASH [17] and IDA [18] nuclear model codes apply Hauser-Feshbach theory for processes in which the compound nucleus decays by fission, and by neutron and γ-ray emission. The coupled-channel optical model [19] within the ECIS [20] code is employed to obtain spin-dependent neutron transmission coefficients and to describe the direct-reaction scattering to low-lying rotational levels. A semiclassical exciton model is used to simulate the preequilibrium particle emission. More computationally-intensive quantum mechanical Feshbach-Kerman-Koonin [21] preequilibrium calculations were also performed at $E_n=14$ MeV incident energy to benchmark the accuracy of the exciton model. Comparisons with neutron spectra from heavy nonfissionable and actinide targets were carried out to validate the magnitude of calculated preequilibrium emission. Continuous level densities were based upon Fermi-gas and constant temperature models, with level density parameters chosen to reproduce *s*-wave level spacings measured at the neutron separation energy. The continuous level density model was matched smoothly onto the experimentally known levels at low excitation. Calculations of effective fission transmission coefficients follow the double-humped fission barrier model by Bjornholm and Lynn [22]; the barrier heights and curvatures were adjusted so as to reproduce the measured (multichance) fission cross section.

A number of differences exist between the GNASH and IDA codes. GNASH calculations of fission included low-lying discrete transition states going over to a continuous level density description whereas IDA included an angular-momentum dependence [23] to the barrier height, based on the rotating liquid drop model. IDA used a Brink-Axel γ-ray strength function [24] in contrast to the model of Kopecky and Uhl [25] implemented in GNASH. The two different GNASH calculations differ in that the first set (GNASH99) uses spin distributions peaked at lower spins compared to the second set (GNASH00) reflecting the small angular momentum transfer that occurs when a preequilibrium particle is emitted. A full description of the details of these calculations will be provided in a forthcoming paper.

The ^{239}Pu$(n,2n\gamma)$ reactions were modeled as follows: the optical model defined an initial composite system spin distribution; neutron emission may occur through either the preequilibrium or compound nucleus mechanism in competition with fission; subsequent neutron decay occurs in competition with fission, leaving a residual nucleus sufficiently low in excitation energy so that it preferentially decays through a γ-ray cascade to the ground state of ^{238}Pu. The portion of the γ-ray cascade with $E_{ex}>E_{cut}$ is modeled using a continuous level density and γ-ray strength function. The part of the cascade with $E_{ex}<E_{cut}$ is carried out using discrete states and branching ratios. $E_{cut}=1.1$ MeV for the GNASH99 calculations. The IDA and the GNASH00 calculations contain 15 additional levels incorporated into the ^{238}Pu level scheme based on a systematic study of low-lying levels in the neighboring isotone ^{236}U and also ^{240}Pu and ^{238}U. E_{cut} was then set at nearly 1.33 MeV.

Figure 2 shows the partial cross sections obtained for the four strongest ^{238}Pu γ rays observed, along with the

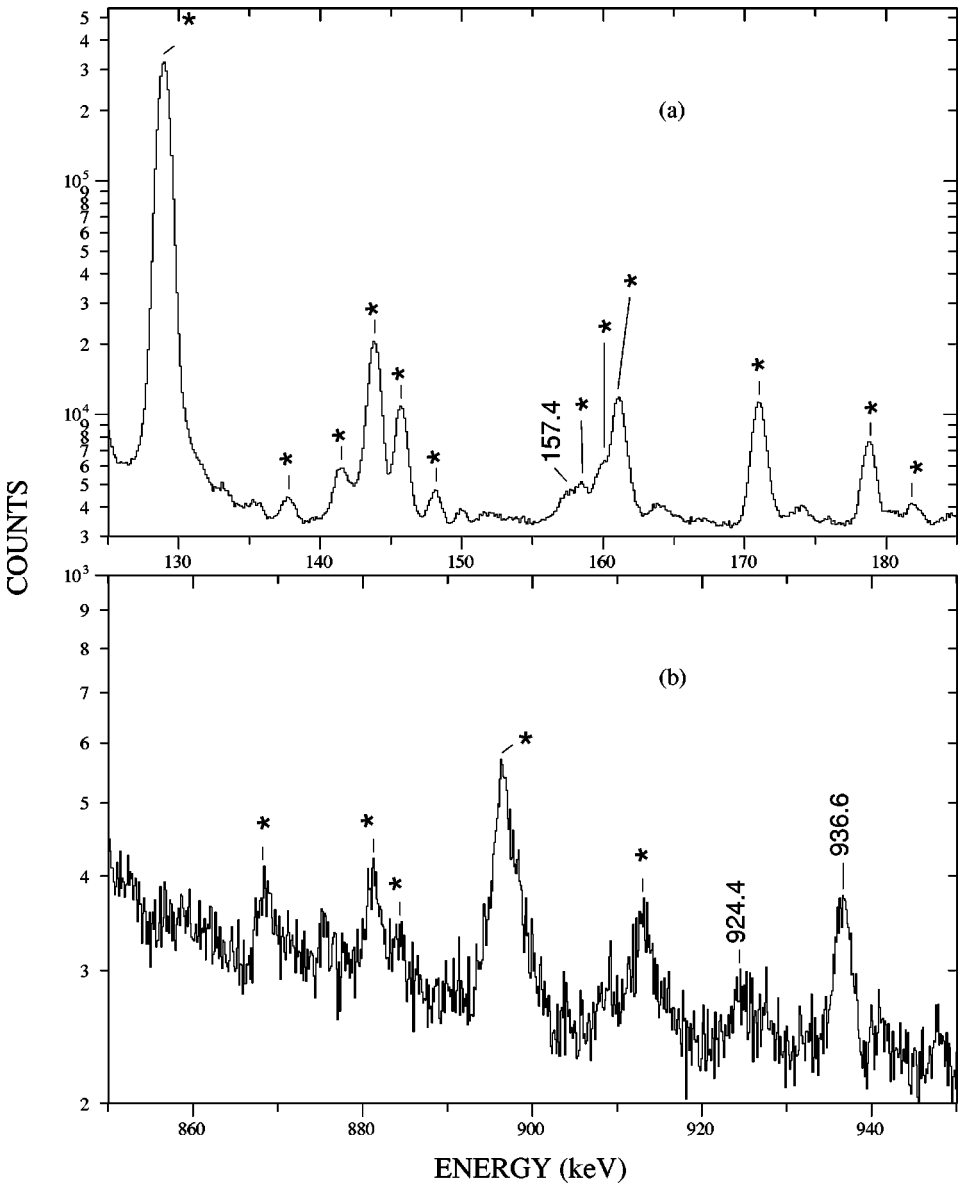

FIG. 1. LEPS spectrum for $E_n = 11.37(45)$ MeV in the γ-ray energy region near the ^{238}Pu yrast $6^+ \rightarrow 4^+$ (top) and the 4_1^- ($E_x = 1083$ keV)$\rightarrow 4^+$ (bottom) transitions. γ rays arising from target radioactivity are marked by an asterisk (*). $(n,2n)$ reaction γ-rays are labeled with their energies.

GNASH99, GNASH00, and IDA calculations scaled to fit the data. The numbers in the insets are the scale factors applied to the model calculations to reproduce the observed partial cross sections. The reaction cross section employed in the GNASH00 calculations was adjusted to reproduce the yrast $6^+ \rightarrow 4^+$ transition. The large differences in magnitude between the observed partial γ-ray cross sections and the other model calculations highlight the fact that any attempt to obtain the channel cross section directly from a model would fail due to the (often large) uncertainties in the reaction cross section.

Another significant discrepancy between the data and the calculations is the difference in the scale factors for the yrast and the off-yrast transitions. For example, the scale factors for the yrast $6^+ \rightarrow 4^+$ and the off-yrast $4^- \rightarrow 4^+$ (in parentheses) transitions for the GNASH00, GNASH99, and IDA calculations are 1.03(0.44), 2.14(0.27), and 2.14(0.90), respectively. These differences suggest problems in the modeling of the γ-ray cascade in the residual ^{238}Pu nucleus. This problem can in turn be attributed to an inaccurate modeling of the spin-energy region populated, or an incomplete or inaccurate continuous γ-ray cascade and/or low-lying discrete level scheme.

The small difference between the scale factors for the two yrast transitions, $(1.12-1.03)/1.03 = 8.7\%$ for the GNASH00 and $(2.31-2.15)/2.15 = 7.4\%$ for IDA indicate that the spin-energy distributions are reasonably well reproduced in both models However, the much larger discrepancy for the GNASH99 $[(3.18-2.14)/2.14 = 48.6\%]$ as compared to the GNASH00 calculations, particularly at higher incident neutron energies, indicates that the preequilibrium spin distribution is more accurately modeled by the lower distributions used in the GNASH00 calculations.

This leaves an incomplete discrete level scheme or an inaccurately modeled continuous γ-ray cascade as a likely cause for the discrepancy in relative intensity between the calculated yrast and off-yrast transitions. The fact that the two calculations using an augmented level scheme (GNASH00

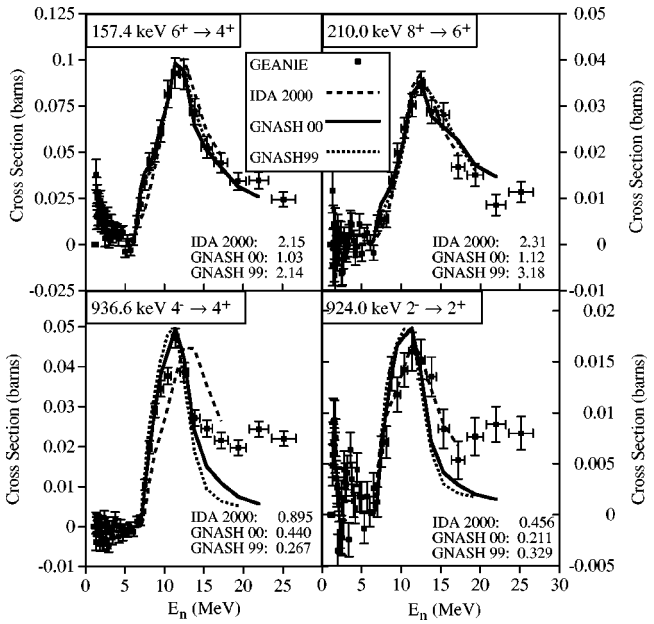

FIG. 2. Partial cross sections for the four strongest transitions in ^{238}Pu observed in the data together with the scaled calculated values from the GNASH99 (dotted line), GNASH00 (solid line), and the IDA (dashed line) model calculations. Numbers in each panel are the scale factors that the model calculations were divided by to best fit the data from 6–20 MeV.

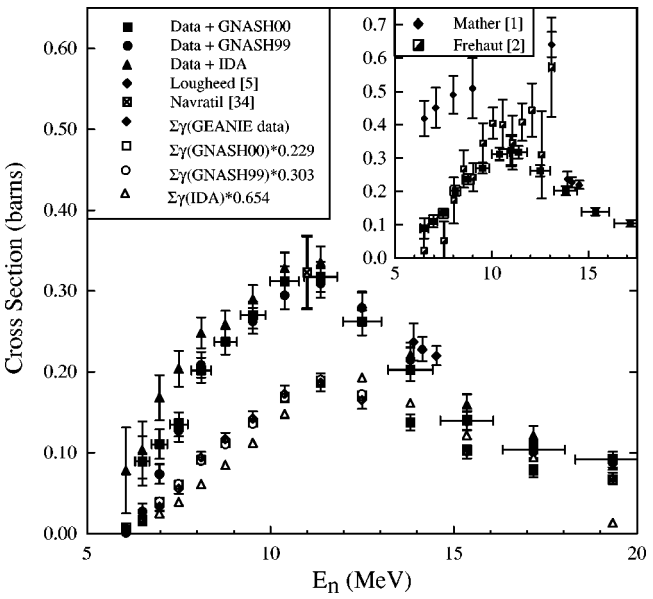

FIG. 3. The γ-ray sum (empty symbols) used to deduce the ^{239}Pu$(n,2n)^{238}$Pu cross section and the deduced cross section (filled symbols) using the two GNASH (squares and circles) and IDA (triangles) reaction models together with the α-decay measurement from Lougheed [3] (diamonds) and the evaluation of actinide $(n,2n)$ cross sections by Navratil *et al.* [27]. The inset shows the values obtained from the GEANIE data with the GNASH00 calculation and data from the earlier measurements by Frehaut [2], Mather [1], and Lougheed [3], and the evaluation by Navratil *et al.* [27].

and IDA) and the calculation made solely with known levels (GNASH99) show the same inability to accurately reproduce the observed yrast vs off-yrast intensities points to the continuous γ-ray cascade used above E_{cut} as the most likely cause.

One possible cause for the poor modeling of the γ-ray cascade above E_{cut} is the lack of nuclear structure information in the continuous level density and γ-ray strength functions. At excitation energies of $E_{cut}=1.33$ MeV (1.1 MeV for the GNASH99 calculations) nuclear structure, such as the projection of the angular momentum onto the symmetry axis of the nucleus K, can play a significant role. In well-deformed nuclei, like ^{238}Pu, K is an approximately conserved quantity. The $J^{\pi}=4_1^-$ level at 1083 keV is the lowest lying $K=4$ bandhead, making it a preferential end-point for high-K cascades. The inability of the models to correctly predict the strong population of this state is expected since the continuous γ-ray cascades do not take K conservation into account. The persistence of K conservation for excitation energies in the range of the continuous γ-ray cascade ($E_x > E_{cut}$) is further supported by recent thermal neutron capture γ-ray data [26].

The lack of detailed nuclear structure information in the models makes any attempt to extract the ^{239}Pu$(n,2n)^{238}$Pu cross section solely from the most intense partial γ-ray cross section (the $6_1^+ \rightarrow 4_1^+$ transition) inappropriate. A successful technique would have to ''add back'' γ-ray intensity that is incorrectly attributed to a different decay path. One such approach involves adding together partial cross sections that populate states that are ''parallel'' (i.e., noncoincident) to each other. This reduces the uncertainties due to missing discrete levels, nuclear structure issues in the statistical cascade (such as K conservation), and spin distributions in the residual nucleus. The transformation equation takes the form

$$\sigma(n,2n)=\sum_{\gamma_i}\sigma^{exp}(n,2n\gamma_i)\times\frac{\sigma^{the}(n,2n)}{\sum_{\gamma_i}\sigma^{the}(n,2n\gamma_i)}. \quad (2)$$

In the case of the Pu data five of the eight observed ^{239}Pu$(n,2n\gamma)^{238}$Pu cross sections are employed; the 157.4 keV $6_1^+ \rightarrow 4_1^+$, the 936.6 keV $4_1^- \rightarrow 4_1^+$, the 918.7 keV $1_1^- \rightarrow 2_1^+$ (corrected for the branching ratio from ENSDF [16]), the 924.0 keV $2_1^- \rightarrow 2_1^+$, and the 617.3 keV $5^- \rightarrow 4^+/3^- \rightarrow 2^+$ doublet. The partial γ-ray sum (for both the data and the model calculations) is shown in Fig. 3. The similarity in shape between the two GNASH calculations suggests that the different preequilibrium spin distributions do not affect the modeled $(n,2n)$ cross section. However, the difference near threshold between IDA and GNASH is more surprising since the compound mechanism, which is dominant in this energy region, is identical in both models. One possible explanation for the difference is the different treatment of fission between the two models since the $(n,2n)$ and the second chance fission channels have the same threshold energy. The ''parallel'' paths approach will fail if (a) there is a strong γ ray that is contaminated by a background line or (b) there are numerous weak decay paths that bypass the transitions used in the sum where the model systematically under- or overpredicts the

γ-ray path intensity. These effects are probably quite small in this case ($<5\%$) based on a comparison of known parallel γ-ray paths.

The ^{239}Pu$(n,2n)$ cross section deduced using all three model calculations is also shown in Fig. 3. The similarity between the cross section extracted using the different calculations suggests that the result is relatively independent of reasonable differences in the low-lying level scheme.

There are two independent checks on this result. (1) The measurement performed near 14 MeV [3] and (2) a cross section deduced from a systematic study of $(n,2n)$ cross sections on other actinides from thorium to uranium [27]. The two points, also plotted in Fig. 3, are consistent with the cross sections obtained in this work. The results of the earlier direct neutron measurements [1,2] are plotted for comparison in the inset of Fig. 3.

In summary, the ^{239}Pu$(n,2n)^{238}$Pu cross section has been deduced using a combination of measured partial cross sections and model calculations. The summation of ''parallel paths'' technique employed produces similar results despite changes in the details of the model (GNASH or IDA) or the low-lying level scheme (measured and extended). The larger than predicted population of the off-yrast high-K states indicates that nuclear structure effects, such as K conservation, could play a significant role in the γ-ray cascade leading to these states.

The authors would like to thank J. D. Anderson, R. Bauer, A. Kerman, F. S. Dietrich, M. A. Ross, G. Reffo, D. Slaughter, D. D. Strottman, and S. A. Wender for support and discussions and the Pu target makers. The technical support of G. Chaparro was essential to this project. This work was funded by the U.S. Department of Energy under University of California Contract Nos. W-7405-ENG-48 (LLNL) and W-7405-ENG-36 (LANL). This work has benefitted from the use of the Los Alamos Neutron Science Center at the Los Alamos National Laboratory. This facility is funded by the U.S. DOE under Contract No. W-7405-ENG-36.

[1] D. S. Mather *et al.,* EANDC(UK) 142-AL, 1972.
[2] J. Frehaut *et al.*, Nucl. Sci. Eng. **74**, 29 (1980).
[3] R. W. Lougheed *et al.* (private communication).
[4] W. Hauser and H. Feshbach, Phys. Rev. **87**, 366 (1952).
[5] D. W. S. Chan, J. J. Egan, A. Mittler, and E. Sheldon, Phys. Rev. C **26**, 841 (1982); G. Reffo, F. Fabbri, K. Wisshak, and F. Kappeler, Nucl. Sci. Eng. **80**, 630 (1982); Z. Sujkowski, D. Chmieleweska, M. J. A. deVoigt, J. F. W. Jansen, and O. Scholten, Nucl. Phys. **A291**, 365 (1977); D. Drake, N. R. Roberson, S. A. Wender, and H. R. Weller, *ibid.* **A410**, 429 (1983); R. Broda, M. Ishihara, B. Herskind, H. Oeschler, and S. Ogaza, *ibid.* **A248**, 356 (1975).
[6] H. Vonach, A. Pavlik, M. B. Chadwick, R. C. Haight, R. O. Nelson, S. A. Wender, and P. G. Young, Phys. Rev. C **50**, 1952 (1994).
[7] P. W. Lisowski, C. D. Bowman, G. J. Russell, and S. A. Wender, Nucl. Sci. Eng. **106**, 208 (1990).
[8] L. A. Bernstein, J. A. Becker, W. Younes, D. E. Archer, K. Hauschild, G. D. Johns, R. O. Nelson, W. S. Wilburn, and D. M. Drake, Phys. Rev. C **57**, R2799 (1998); P. E. Garrett *et al.*, *ibid.* **62**, 054608 (2000).
[9] J. C. Lashley, M. S. Blau, K. P. Staudhammer, R. A. Pereyra, J. Nucl. Mat. C **274**, 315 (1999); J. C. Lashley *et al.,* Purified Plutonium Reduces Background Interference in Nuclear Cross-Section Measurements, LALP-00-104, 2000, available at http://lansce.lanl.gov/research/pdf/Pu.pdf
[10] J. F. Briesmeister, MCNP—A General Monte Carlo *N*-Particle Transport Code, Technical Report No. LA-12625-M, LANL, 1997.
[11] D. P. McNabb *et al.,* Uncertainty Budget and Efficiency Analysis for the ^{239}Pu$(n,2n)$ Reaction Cross Section Measurements, UCRL-ID-139906.
[12] S. P. Simakov, A. Pavlik, H. Vonach, and S. Hlavac, IAEA Nuclear Data Section IDC(CCP)-413, 1998.
[13] L. A. Bernstein *et al.,* Measurement of Several ^{239}Pu(n,xn) Partial γ-ray Cross Sections for $x\leqslant 3$ Using GEANIE at LANSCE/WNR, UCRL-ID-140308.
[14] D. C. Radford, RADWARE analysis package as maintained at radware.phy.ornl.gov
[15] ENDF/B-VI evaluation, MAT 9228, revised 5 November 1998; data retrieved from the ENDF database (http://www.nndc.bnl.gov/); P. W. Lisowski, Los Alamos National Laboratory (private communication).
[16] Data extracted using the NNDC On-line Data Service from the ENSDF and EXFOR databases, file revised as of 07/17/00; M. R. Bhat, in *Evaluated Nuclear Structure Data File (ENSDF), Nuclear Data for Science and Technology*, edited by S. M. Qaim (Springer-Verlag, Berlin, 1992), p. 817.
[17] P. G. Young, E. D. Arthur, and M. B. Chadwick, in Comprehensive Nuclear Model Calculations: Theory and Use of the GNASH Code, Proceedings of the IAEA Workshop on Nuclear Reaction Data and Nuclear Reactors—Physics, Design, and Safety, Trieste, Italy, 1996, edited by A. Gandini and G. Reffo, pp. 227–404.
[18] G. Reffo and F. Fabbri, IDA system of codes (unpublished).
[19] P. G. Young and E. D. Arthur, in *Theoretical Analyses of (n,xn) Reactions on ^{235}U, ^{238}U, ^{237}Np, ^{239}Pu, Proceedings of Nuclear Data for Science and Technology*, Jülich, Germany, 1991, edited by S. Qaim (Springer-Verlag, New York, 1992).
[20] J. Raynal, code ECIS95 (unpublished).
[21] H. Feshbach, A. Kerman, and S. Koonin, Ann. Phys. (N.Y.) **125**, 429 (1980).
[22] S. E. Bjornholm and J. E. Lynn, Rev. Mod. Phys. **52**, 725 (1980).
[23] A. J. Sierk (private communication).
[24] D. M. Brink, D. Phil. thesis, University of Oxford, 1955; P. Axel, Phys. Rev. **126**, 671 (1962).
[25] J. Kopecky and M. Uhl, Phys. Rev. C **41**, 1941 (1990).
[26] I. Huseby, T. S. Tveter, L. Bergholt, M. Guttormsen, E. Melby, J. Rekstad, S. Siem, and R. K. Sheline, Phys. Rev. C **55**, 1805 (1997).
[27] P. Navratil and D.P. McNabb, UCRL-ID-140697.